

Modeling Procedures For Breast Cancer Diagnosis Based On Clinical Elastography Images

Mohamed A. Naser
Biomedical Engineering
Department
Minia University,
Minia, Egypt,
madian033@yahoo.com

Ahmed M. Sayed
Biomedical Engineering
Department
Helwan University
Helwan, Egypt
a.sayed@h-
eng.helwan.edu.eg

Ashraf A. Wahba
Biomedical Engineering
Department
Helwan University
Helwan, Egypt
ashraf_wahba@h-
eng.helwan.edu.eg

Mohamed A. A.
Eldosoky
Biomedical Engineering
Department
Helwan University
Helwan, Egypt
hm.eldosoky@gmail.com

Abstract: Nowadays, breast cancer is considered the second cause common cancer type of women death. To determine the proper therapeutic procedures before cancer spreading, early detection of cancer is a definitive step. Ultrasound elastography is considered one of the early effective noninvasive diagnostic tools. It has many advantages as low cost, its safety and the highly increasing development in various medical imaging applications.

In this work, 3D modelling and simulations using virtual phantoms that were designed based on realistic in-vivo experimental results. The models were constructed for each in-vivo individual case assuring the biomechanical features of the breast tissue. The models are integrated several breast tumor's parameters including size, shape, and position. In particular, mathematical and computational analyses were used to compare this work's results by assorted specifics of in-vivo elastograms. Tumor discrimination; either malignant or benign, was performed depending on the non-linear biomechanical properties of breast tumors. To calculate the main classification parameters, tissue deformations and strain differences among the suspected mass and the normal surrounding background tissue were analyzed and empirically fitted. The results show a kindly agreement between the model outputs and the in-vivo diagnostics elastograms. Generally, the introduced finite element modeling method can be considered as a non-invasive diagnostic procedure in an early stage to preceding classify breast tumors. The 3D simulation results can assure a more theoretical insight on the behavior of nonlinear biomechanical properties that might not be obvious or convenient using clinical experimentations.

Keywords—*Cancer Detection; Breast Tumors; Elastography; Tissue deformation; 3-D finite element.*

I. INTRODUCTION

At present, breast cancer has become a danger threat for women. Worldwide, it is being considered as the second cause for disease founded in women [1]. Once it is founded, the condition becomes life-threatening, as defective cells can extend rapidly to other organ in the body. Therefore, early and accurate detection of cancer become an insistent priority procedure followed by the appropriate therapeutic steps [2]. Although biopsy is considered as the gold-standard step for pathological evaluation of breast diseases, yet it is an invasive, inconvenient and costly technique. It turns out that other noninvasive detection techniques might be alternative methods such as Ultrasound (US), mammography, and magnetic resonance imaging (MRI) [3]. One of the valuable early breast cancer diagnosis tools is the elastography, based on ultrasound imaging technique. It has many priorities as a noninvasive tool; its safety, low cost and the amazing development in the imaging sectors.

Despite that fact, it isn't as yet well-considered as a dependable reliable tool to decrease reliance on biopsies in accurately classifier the nature of breast lesions.

At the beginning of 1990s, elastography was progressing to improve the ultrasound imaging technique to the functional grade [4-6]. 3-D finite element (FE) in ultrasound imaging has the possibility to be a modeling tool to enhance the effectiveness of tissue classification noninvasively. It can be applied to reinforce our conception about the differentiation process between breast tissue masses [7].

Imaging and mapping the biomechanical characteristics of biological tissues have become the pivotal point of many researchers [8, 9]. Many studies depended on tissues elasticity imaging. They have confirmed that hypothesis, such as those concerned with breast cancer detection algorithms using ultrasound-based approaches [10-13]. The major objective of those works mainly based on approaching to map some biomechanical properties of tissues aiming to provide important clinical information in an anatomically significant method.

Changeable stiffness of biological tissue behavior can be considered as a symptom of an abnormality. Nonlinearity acts as the corner stone of developing the diagnostic power of elastography in the most clinical and pre-clinical applications, [14]. Therefore imaging the non-linearity parameters of biomechanical behavior, specifically related to its elasticity, assigns a functional biomarker for early diagnosis of defective tissues[15].

Finite element modeling (FEM) is playing the backbone in several fields. Nowadays, several powerful packages software, as ANSYS, can perform complicated simulation with highly deformations. Many researchers have demonstrated how was FEM is a successful method in modeling the highly deformation of soft tissue. Modeling breast masses took considerable attention based on various diagnostic modalities such as magnetic resonance imaging (MRI) data [16-18], elastography [19-21] and biopsy [22].

This work illustrates how functionality of FEM may be used in breast tumor analysis to estimate biomechanical parameters as accurate as possible, aiding for early masses classification, and consequently, cancer diagnosis. In this work, a 3D FEM for the breast models constructed depending on realistic data for a number of 4 clinical cases are introduced, with typical dimensions, changeable material properties, boundary conditions and loads. Models outcomes are compared with an earlier clinically and pathologically data, verified using biopsies technique, previously imaged by 3D ultrasound elastography. Generated parameters from ultrasound elastography

imaging were fed and applied in the hypothesized models which results are discussed later.

II. METHODOLOGY

A. Model Construction

The mainly concept of elastography is based on using the ultrasound probe as a compression tool and an imaging tool on the breast at the same time. Generally, breast tumors diagnosis in elastography based on tissue elasticity behaviors that indicated mainly on strain images. They are obtained mathematically by calculating the derivative of tissue deformation occurring along US beam.

The 3D model has been designed using ANSYS software package (ANSYS, Inc., Canonsburg, PA, USA). Three idealistic steps summarize the fundamentals of FEM analysis [23].

Step 1: Preprocessing; building geometry, representing material properties, element meshing and applying boundary conditions and loads.

Step 2: Analysis; the formulated equations are formed to appoint the field variation.

Step 3: Post processing; calculating and displaying graphical result of variables.

Using the following conditions, 4 models are built for 4 clinical breast tumors cases with different positions, sizes, and material behaviors for either 2 cases of fibrocystic change as benign and 2 cases of invasive ductal carcinoma as a malignant masses characteristic, as indicated in previously reported studies [24, 25].

B. Design modeling and governing equations

Four clinically and pathologically diagnosed breast mases were diagnosis using 3D elastogram. Parameters, listed in Table I used in building geometric model for each individual case based on available data. The same geometric dimension in the designed model for the whole breast in all concerned cases is used, for simplicity, while the inner sizes of masses and its surrounding normal tissues are changeable according to available clinical data of each case [25]. Fig. 1 illustrates the 3-D model structural design modeler using ANSYS.

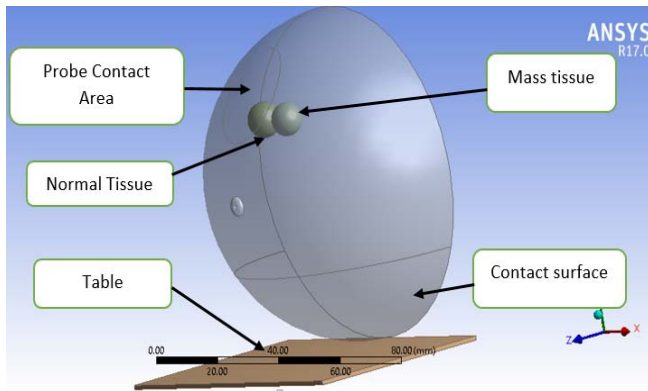


Fig. 1. 3D FE model of breast.

TABLE I. DIMENSIONS USED IN THIS STUDY.

Geometry	Values
Breast radius	50 mm
Normal gland radius	1.5 ~ 3.85 mm
Benign radius	1.57 and 3.81 mm
Malignant radius	1.98 and 3.82 mm
Surface area of contact probe	619.21 mm ²

The main idea of FE analysis is to divide the geometry into small elements dealing with each element algebraically using the linear equation “(1),” that represents the biomechanical proprieties of elements behavior in matrix shape, as follows:

$$[F] = [K][U] \quad (1)$$

while $[F]$ is all external applied forces, $[K]$ is the element stiffness matrix, and $[U]$ is the nodal displacements. During the solution step the software, mathematically calculates nodal displacements $[U]$, which are the primary calculated variables of the model output.

C. Modeling non-linear biomechanical material proprieties

The FEM method was used in that problem as it has the capability for simulation the biomechanical behaviors. Generality, the majority of the biomechanical proprieties of biological tissues combine the behavior of both a viscous and elastic responses. So, designing the model was based on the following assumptions:

- Homogeneous [26].
- Isotropic [22, 27].
- Incompressible material [28].
- Non-linear elastic properties with exponential stress-strain relationship for the breast tissues [15, 28-30].
- No temperature effects are included in the model.

Fig. 2 shows the main concept of how elastography technique helps in differentiation under compression force based on the highly changeable of biomechanical proprieties (specifically stiffness) $[b^*, m^*]$ of normal and abnormal tissues as included in Table II. Equation (2) represents the non-linear exponential stress-strain relationship for the itemized tissues in our model.

$$\sigma_n^* = \frac{b^*}{m^*} (e^{m^* \epsilon_n} - 1) \quad (2)$$

TABLE II. BIOMECHANICAL PROPRIETIES OF BREAST TISSUES.

Material name	b^*	m^*
Normal gland	15174.5	12.3
Fibro adenoma	37572.4	20.0
Infiltrating Ductal Carcinoma (IDC)	37958.7	19.9

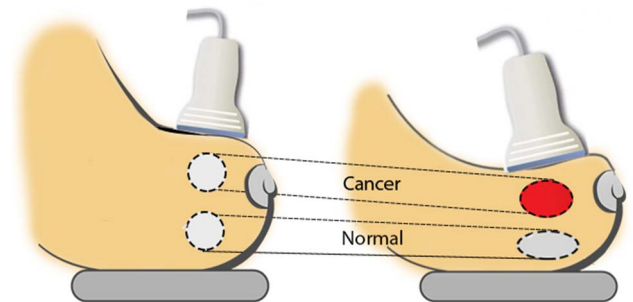


Fig. 2. Breast deformation under pressure force.

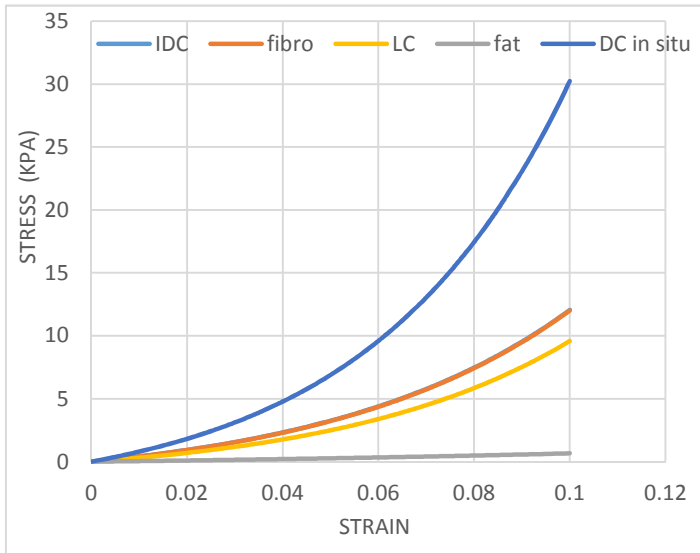


Fig.3. Regenerated curves of material proprieties.

The exponential equation “(2),” allows to redraw the stress-strain relationship for all tissues included in Table II. The constants b^* and m^* determine the biomechanical behavior of each material. Fig. 3 shows the stress-strain curves for the tissue material, which was redrawn based on a previously reported study [15].

D. 3-D Modeling procedures

While, the biomechanical behaviors of breast tissues are described as a nonlinearity, hyperplastic material is an idealistic simulation of stress-strain relationship for that types of tissues [15]. Therefore, several strain functions can be used to simulate the nonlinear behavior of highly deformation behavior inside the breast [31].

The model implements the following assumptions:

- In agreement with the static structural as a physics of the problem.
- Axisymmetric 3D degrees of freedom.
- The breast tissue was modeled as one homogeneous layer.
- Hyperelastic material described by exponential elastic stress-strain relationship for the breast.
- The geometry is meshed with 3-D tetrahedral and 10-node Structural Solid 148 is used to fill out the designed

geometry. Is considered the preferred element type to satisfy our main behavior here that is deflection.

-Nonlinear adaptive region processes are activated, so remeshing was used to refine the model.

Generally, the block diagram in Fig. 4 illustrates the analysis process sequences in ANSYS 17 software and shows the modality of the proposed algorithm. As shown, the problem is stated as a static structural problem. Then, constructing the geometry file using static structural-design modeler. Every tissue is assigned by its material propriety. The material behavior is defined inside the software as a Hyperelastic material. Then a proper element type is chosen in the meshing step. The efficiency of model success depends on the meshed elements typeset in terms of its size and fitness to the breast that is tested and checked. After that, a contact pair is created between the surface's elements of the breast and the fixed support table, and must guarantee preventing overlap between both target and contact elements, breast and the table respectively, (contact pair) and allow sliding between the closed surfaces at the same time. Fixed boundary conditions are stated at the rib cage and fixed support table. Activation frictional contact is very essential to avoid expected penetration with a friction coefficient of 0.001[7] and activation Augmented Lagrange algorithm.

Standard Earth Gravity is activated beside three pre-compression loads in the load and boundary conditions phase. Thus the solution step is begun by applying “(1),” and nodal displacements are calculated. Subsequently, the graphical results are presented and checked related to nodal strain values to be logically acceptable as shown in Fig. 5. The corrected nonlinear power parameter is then calculated from force – strain difference curve fitted and compared with a reference in-vivo power parameter. If the results are unacceptable, we must get back to the ‘geometry’ step, and make necessary adjustments.

E. Boundary conditions and Loads

A contact area is formed between the breast and the probe where the uniaxial compression force is aligned on the mass orientation during imaging procedures named probe contact area. It can be modeled as frictionless as it extends no friction which covered by gel. Highly and

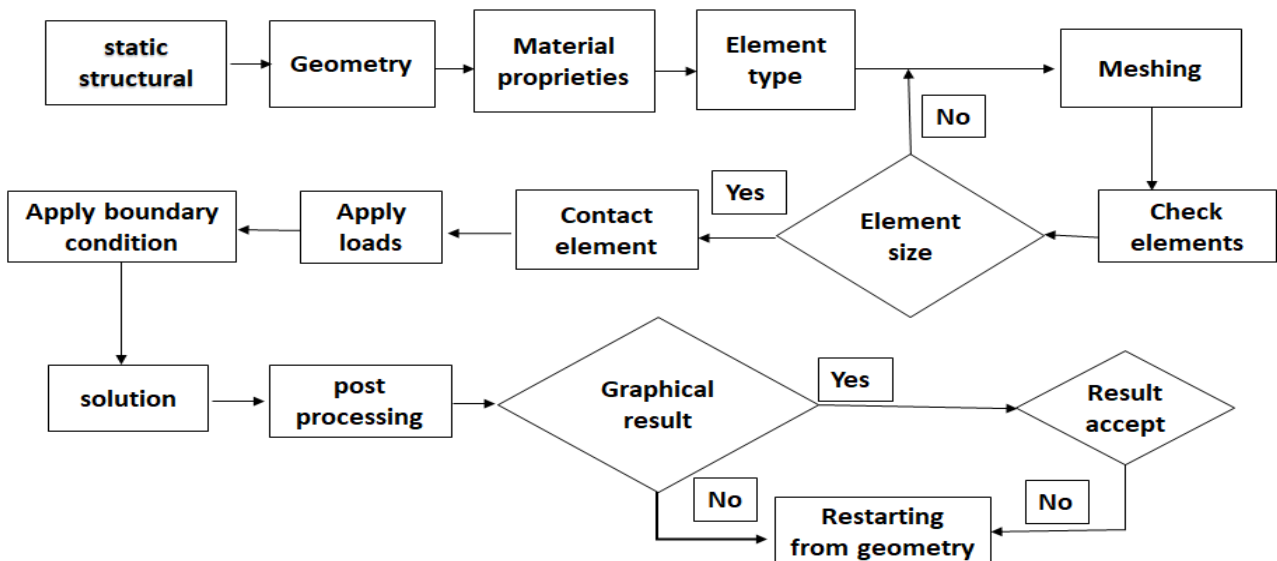


Fig.4. Block diagram of breast model.

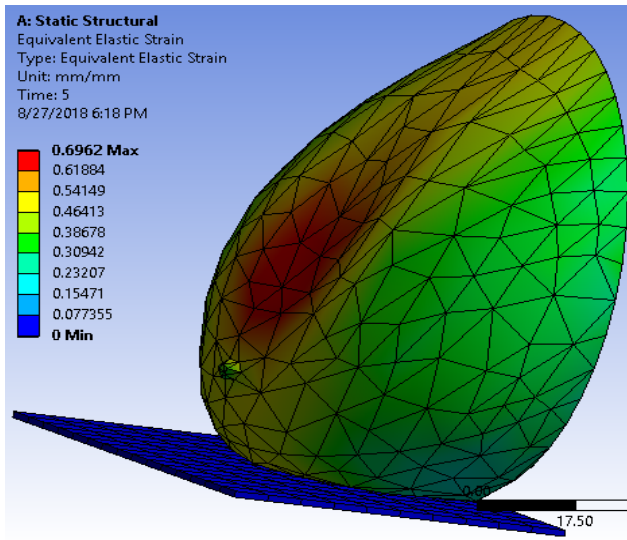


Fig.5. Elastic strain of breast model.

rapidly deformation can happen abruptly, so the multi force in the boundary condition is divided to five steps to illustrate more clinical information about the study case. The force steps are 5N, 10N, 20N, 30N, 40N (Newton).

F. Mass classification technique

This research paper based on calculating the non- linear power equation coefficient n , as shown in “(3)”, as the classifier parameter for breast cancer diagnosis, [15, 24, 25]. As a result of the more compression they are exposed to, tumors behave a higher stiffness. Then the curve fitting method is utilized to fit a nonlinear power – law relationship of strain difference curve versus multi-forces for each case as follows:

$$f = m(\Delta\epsilon)^{\frac{1}{n}} \quad (3)$$

where f is the multi compressed force. $\Delta\epsilon$ act as the strain difference between the mass and its normal surrounding tissue. We mainly focus through this work on the parameter n for breast masses classification. The introduced technique depends on comparing the reference n calculated in [24] with our calculated non- linear parameter n . The main idea of elastography is when increasing the compression force, the stiffness of malignant tumors increases speedily compared with benign tumors stiffness. The mainly introduced modeling method of mass classifier technique, based on quantifying the non-linearity phase of the suspected tissues. If high degrees of the nonlinearity coefficient n ($n > 1$) is found, this displays a malignant behavior.

Fig. 6 explains obviously how the strain difference rate are rising exponentially with the pre-compression forces marked with $f = 2, 3$, and 4 kgf. After that, the difference between the tumor strain and its normal background soft tissue strain is calculated at each level of force which that increases exponentially with applied force level.

III. RESULTS

Fig. 5 illustrates the style of the graphical results of the strain profile of the breast model. The scale result has a wide range from min value represented as a blue color, stiffer, and the max value represented as red color, low stiffer. Table III displays the graphical results of FE simulation illustrating 3 points curve and full scale curve

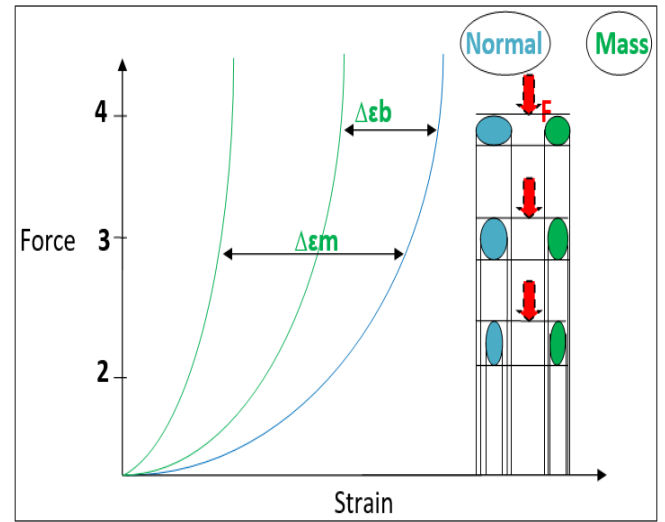


Fig.6. Force-strain curves under multi compression [with permission].

for 4 clinical cases (2 benign and 2 malignant). The results are calculated and fitted according to the nonlinear equation “(3)”. The mainly concept for classifier way is that if $n < 1$, the case is benign case and if $n > 1$, the case is malignant case.

A. Benign Cases:

Following the pre-described modeling methods in FEM from Table III-A for a breast masses of patient #6 and patient #7 as the volume is 231.67 and 16.10 mm³ respectively, based on the volume segmentation that considered as a ball. From the output model parameters of patient #6, FEM n is 0.211 by 3 values and is $n = 0.398$ by full range which around closely by In- vivo n is 0.229, showing a malignant behavior is found. From the output model parameters of patient #7, FEM n is 0.212 by 3 values and is 0.363 by full range which around closely by In- vivo n is 0.269, showing a malignant behavior is found. Based on that results, it is a good match between FEM modeling results and the real clinical data.

B. Malignant Cases:

Following the pre-described modeling methods in FEM from Table III-B for a breast masses of patient #2 and patient #10 as the volume is 235.10 and 624.60 mm³ respectively, based on the volume segmentation considered as a ball. From the output model parameters of patient #2, FEM n is 1.745 by 3 values and is 1.387 by full range which around closely by In- vivo n is 1.696, showing a malignant behavior is found. From the output model parameters of patient #10, FEM n is 2.237 by 3 values and is 1.39 by full range which around closely by In- vivo n is 1.981, showing a malignant behavior is found. Based on that results, it is a good match between FEM modeling results and the real clinical data.

V. DISCUSSION

FEM is one of the most popular numerical simulation methods can solve and predict the behavior of any system depending on experimental data based on specific governing equations. Today, it is noticed that the highly developing in the hardware sector the more powerful processors are generated. So, proceeding highly

simulations with multi degrees of freedom of several complex models will become very precision.

In this study, a full range of applied force beginning from 0 value to 4 kgf is divided to 53 sub steps from 5 steps during examination time giving more details of clinical information. The FE analysis calculates the strain difference versus multi divided force at each step level as shown in Table III. The essential aim of usage the derived strains, especially von mises strain, is to predict the yielding of materials under uniaxial compression force. The curves in benign cases exhibited a relatively higher slope than the curves in malignant cases. That orientation reflects the non-linear mechanical behavior of the malignant tissues, wherein the more stress they exposed to, the higher stiffness they display.

In this work, FEM technique is used to design 3D virtual phantom that allow applying multi- compression forces to calculate the non-linear parameter.

This way displays a diagnostic tool for more delicate evaluations. The actual maximum compression load is restricted by the patient's ability to afford more compression without feeling extra pain.

Those models are fitted according a non-linear power equation (3), get the values of the nonlinear parameter (n). Table III shows the calculated data comparing between in-vivo elastography [25] and the results of this study.

From one side, according to the introduced work, that detection technique is verified [25]. It depends only on the nonlinear biomarker of the real clinical cases that has several limits. On the other side, this paper results encourage to continue using FE modeling in further more in vitro experimental cases.

While this paper concentrates only on the non-linear biomarker n for tissue classification algorithm. As a result of FE, with no limits, it gives a chance to study new biomarkers to get closer of tissue discrimination. The nonlinear parameter m and US probes' temperature effect can be included in another future work.

IV. CONCLUSIONS

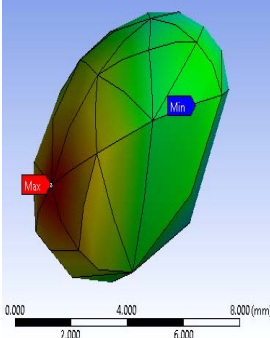
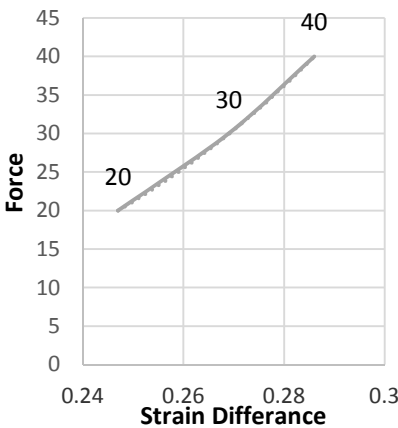
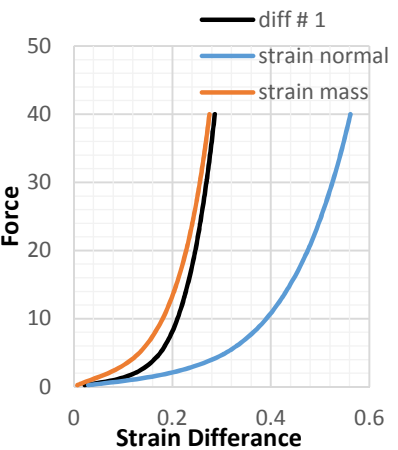
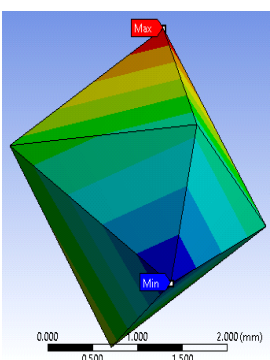
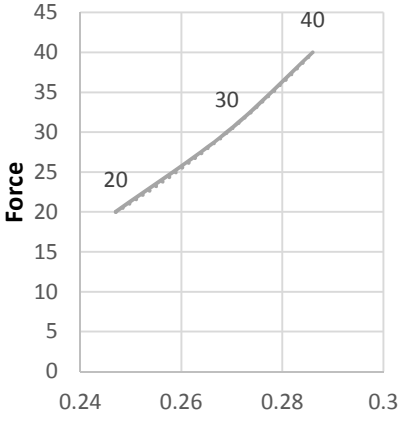
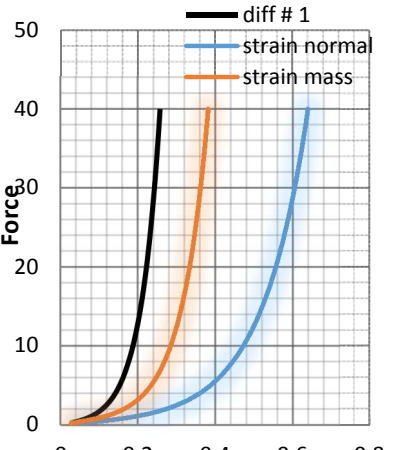
According this research paper, FEM can be considered as a good tool to enhance the vision about the elastography imaging in breast cancer diagnosis, illustrating the importance of the elasticity as a biomarker for breast masses detection. These virtual models can be considered as phantoms that can help in accurate decision about the nature of suspected tissues according the biomechanical effects under the applied force steps in multi directions. The FE results agreed well to a very good extent with the in-vivo experimental cases. This work is restricted by the few number of breast tumors cases inserted, so the specificity and sensitivity of the masses detection algorithm are not reported, that would not show the actual performance appraisal of the tool in such a case. It is hypothesized FEM would potentially fetch us nearly to increase the accurate diagnostic decision and minimize the usage of biopsy in breast cancer characterization. In the future work, it is hoped to promote more functionality of FEM algorithm in the breast cancer diagnostic, depending on real experimental data generated by many imaging tools such as MRI or US. It is a potential conception to construct 3-D FEM models based on DICOM images that can be formed from many software packages as 3-d doctor and applying the presented description technique in this work.

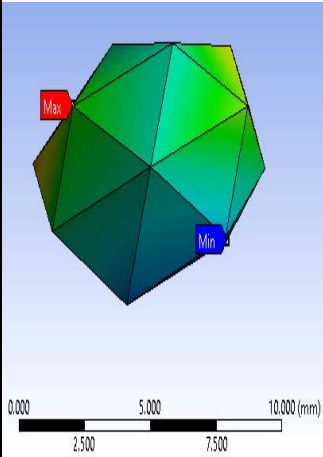
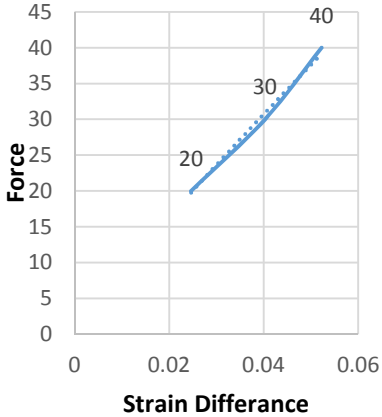
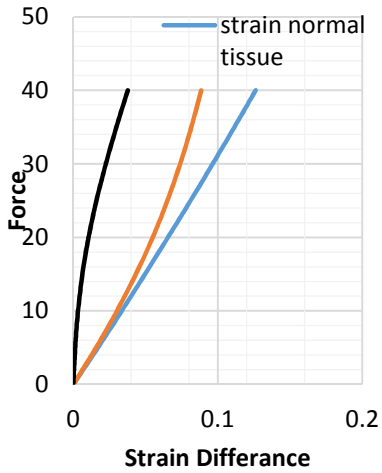
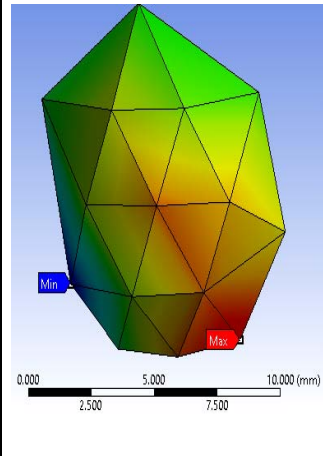
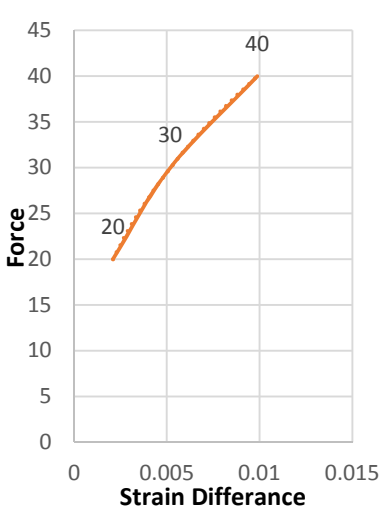
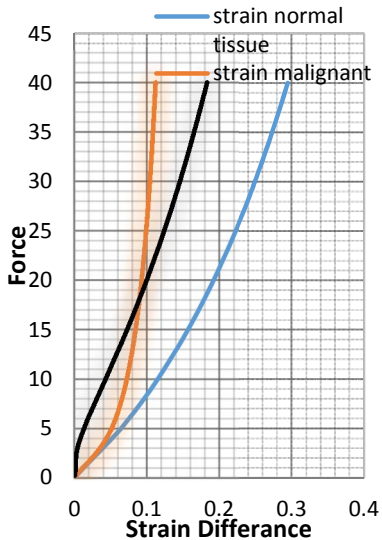
References

- [1] (American Cancer Society 2017). *Cancer Facts & Figures 2017*. Available: <https://www.cancer.org/cancer/breast-cancer.html>
- [2] N. G. Ramiao, P. S. Martins, R. Rynkevicius, A. A. Fernandes, M. Barroso, and D. C. Santos, "Biomechanical properties of breast tissue, a state-of-the-art review," *Biomech Model Mechanobiol*, vol. 15, no. 5, pp. 1307-23, Oct 2016.
- [3] T. V. N. R. A. Govardhan, "Classical and Novel Diagnosis Techniques for Early Breast Cancer Detection—A Comparative Approach," *International Journal of Engineering Mathematics and Computer Sciences*, vol. 3, no. 11, pp. 12-16, 2015.
- [4] M. O'Donnell, A. R. Skovoroda, B. M. Shapo, and S. Y. Emelianov, "Internal displacement and strain imaging using ultrasonic speckle tracking," *IEEE transactions on ultrasonics, ferroelectrics, and frequency control*, vol. 41, no. 3, pp. 314-325, 1994.
- [5] J. Ophir, I. Cespedes, H. Ponnekanti, Y. Yazdi, and X. Li, "Elastography: a quantitative method for imaging the elasticity of biological tissues," *Ultrasonic imaging*, vol. 13, no. 2, pp. 111-134, 1991.
- [6] R. M. Lerner, K. J. Parker, J. Holen, R. Gramiak, and R. C. Waag, "Sono-elasticity: medical elasticity images derived from ultrasound signals in mechanically vibrated targets," in *Acoustical imaging*: Springer, 1988, pp. 317-327.
- [7] S. Celi, F. Di Puccio, and P. Forte, "Advances in finite element simulations of elastosonography for breast lesion detection," *Journal of biomechanical engineering*, vol. 133, no. 8, p. 081006, 2011.
- [8] J. Ophir *et al.*, "Elastography: imaging the elastic properties of soft tissues with ultrasound," *Journal of Medical Ultrasonics*, vol. 29, no. 4, pp. 155-171, 2002.
- [9] L. Gao, K. Parker, R. Lerner, and S. Levinson, "Imaging of the elastic properties of tissue—A review," *Ultrasound in medicine & biology*, vol. 22, no. 8, pp. 959-977, 1996.
- [10] K. M. Hiltawsky, M. Krüger, C. Starke, L. Heuser, H. Ermert, and A. Jensen, "Freehand ultrasound elastography of breast lesions: clinical results," *Ultrasound in Medicine and Biology*, vol. 27, no. 11, pp. 1461-1469, 2001.
- [11] J. Bercoff *et al.*, "In vivo breast tumor detection using transient elastography," *Ultrasound in Medicine and Biology*, vol. 29, no. 10, pp. 1387-1396, 2003.
- [12] A. Itoh *et al.*, "Breast disease: clinical application of US elastography for diagnosis," *Radiology*, vol. 239, no. 2, pp. 341-350, 2006.
- [13] D. M. Regner *et al.*, "Breast lesions: evaluation with US strain imaging—clinical experience of multiple observers," *Radiology*, vol. 238, no. 2, pp. 425-437, 2006.
- [14] T. A. Krouskop, T. M. Wheeler, F. Kallel, B. S. Garra, and T. Hall, "Elastic moduli of breast and prostate tissues under compression," *Ultrasonic imaging*, vol. 20, no. 4, pp. 260-274, 1998.
- [15] P. Wellman, R. D. Howe, E. Dalton, and K. A. Kern, "Breast tissue stiffness in compression is correlated to histological diagnosis," *Harvard BioRobotics Laboratory Technical Report*, pp. 1-15, 1999.
- [16] D. B. Plewes, J. Bishop, A. Samani, and J. Sciarretta, "Visualization and quantification of breast cancer biomechanical properties with magnetic resonance elastography," *Physics in medicine and biology*, vol. 45, no. 6, p. 1591, 2000.
- [17] A. M. Sayed, E. Zaghoul, and T. M. Nassef, "Automatic Classification of Breast Tumors Using Features Extracted from Magnetic Resonance Images," *Complex Adaptive Systems*, vol. 95, pp. 392-398, 2016.
- [18] M. Z. Unlu *et al.*, "Computerized method for nonrigid MR-to-PET breast-image registration," *Computers in biology and medicine*, vol. 40, no. 1, pp. 37-53, 2010.
- [19] S. Misra, K. Ramesh, and A. M. Okamura, "Modeling of Tool-Tissue Interactions for Computer-Based Surgical Simulation: A Literature," 2008.
- [20] J. op den Buijs, H. H. Hansen, R. G. Lopata, C. L. de Korte, and S. Misra, "Predicting target displacements using ultrasound elastography and finite element modeling," *IEEE Transactions on Biomedical Engineering*, vol. 58, no. 11, pp. 3143-3155, 2011.

- [21] A. A. Wahba, N. M. M. Khalifa, A. F. Seddik, and M. I. El-Adawy, "A Finite Element Model for Recognizing Breast Cancer," *Journal of Biomedical Science and Engineering*, vol. 07, no. 05, pp. 296-306, 2014.
- [22] F. S. Azar, D. N. Metaxas, and M. D. Schnall, "A finite element model of the breast for predicting mechanical deformations during biopsy procedures," in *Mathematical Methods in Biomedical Image Analysis, 2000. Proceedings. IEEE Workshop on*, 2000, pp. 38-45: IEEE.
- [23] A. A. H. Sayed, N. H. Solouma, A. A. El-Berry, and Y. M. Kadah, "Finite Element Models for Computer Simulation of Intrastromal Photorefractive Keratectomy," (in English), *Journal of Mechanics in Medicine and Biology*, vol. 11, no. 5, pp. 1255-1270, Dec 2011.
- [24] A. Sayed, G. Layne, J. Abraham, and O. Mukdadi, "Nonlinear characterization of breast cancer using multi-compression 3D ultrasound elastography in vivo," *Ultrasonics*, vol. 53, no. 5, pp. 979-991, 2013.
- [25] A. Sayed, G. Layne, J. Abraham, and O. M. Mukdadi, "3-D visualization and non-linear tissue classification of breast tumors using ultrasound elastography in vivo," *Ultrasound in medicine & biology*, vol. 40, no. 7, pp. 1490-1502, 2014.
- [26] A. Sarvazyan *et al.*, "Biophysical bases of elasticity imaging," in *Acoustical imaging*: Springer, 1995, pp. 223-240.
- [27] W. Hayes, L. Keer, G. Herrmann, and L. Mockros, "A mathematical analysis for indentation tests of articular cartilage," *Journal of biomechanics*, vol. 5, no. 5, pp. 541-551, 1972.
- [28] Y.-c. Fung, *Biomechanics: mechanical properties of living tissues*. Springer Science & Business Media, 2013.
- [29] F. S. Azar, D. N. Metaxas, and M. D. Schnall, "A finite element model of the breast for predicting mechanical deformations during biopsy procedures," pp. 38-45, 2000.
- [30] M. Zhang, Y. Zheng, and A. F. Mak, "Estimating the effective Young's modulus of soft tissues from indentation tests—nonlinear finite element analysis of effects of friction and large deformation," *Medical engineering & physics*, vol. 19, no. 6, pp. 512-517, 1997.
- [31] J. H. Hipwell, V. Vavourakis, L. Han, T. Mertzaniidou, B. Eiben, and D. J. Hawkes, "A review of biomechanically informed breast image registration," *Physics in medicine and biology*, vol. 61, no. 2, p. R1, 2016.

TABLE III. CLINICAL TUMORS ANALYSIS USING FEM

A- Benign Cases			
Mass strain	Strain Difference normal-mass (3 force level data)	Strain Difference normal-mass (All force level data)	Notes (benign cases)
			Patient #6 In-vivo n=0.229 3 points $y = 14913x^{4.7296}$ FEM n=0.211 Full scale $y = 1127.6x^{2.322}$ FEM n=0.431
			Patient #7 In- vivo n=0.269 3 points $y = 24257x^{4.7244}$ FEM n=0.212 Full scale $y = 1265.1x^{2.7548}$ FEM n=0.363

B- Malignant Cases			
Mass strain	Strain Difference normal-mass (3 force level data)	Strain Difference normal-mass (All force level data)	Notes (malignant cases)
			Patient#2 In- vivo n=1.696
			3 points $y = 193.17x^{0.5731}$ FEM n=1.745
			Full scale $y = 479.17x^{0.7208}$ FEM n=1.387
			Patient #10 In- vivo n=1.981
			3 points $y = 14.91x^{0.4469}$ FEM n =2.237
			Full scale $y = 122.21x^{0.718}$ FEM n=1.39